Biointerface Research in Applied Chemistry
Open-Access Journal (ISSN: 2069-5837)

Article
Volume 14, Issue 4, 2024, 88
https://doi.org/10.33263/BRIAC144.088

Adsorption Studies of Imidacloprid from Aqueous Solution using Polyacrylamide Coated Magnetite Nanoparticles as a Potential Nanoadsorbent

Keerti Rani [1], Ramesh Kumar [1,*], Devender Singh [2], Harish Kumar[3], Parvin Kumar [1], Suresh Kumar [1]

[1] Department of Chemistry, Kurukshetra University, Kurukshetra (Haryana), 136119, India; keertiattri1540@gmail.com (K.R.), rameshkumarkuk@gmail.com (R.K.), parvinchem@kuk.ac.in (P.K.), duaskchem@gmail.com (S.K.);
[2] Department of Chemistry, Maharshi Dayanand University, Rohtak (Haryana), 124001, India; devjakhar@gmail.com (D.S.);
[3] Department of Chemistry, School of Basic Sciences, Central University of Haryana, Mahendergarh (Haryana) 123031, harishkumar@cuh.ac.in (H.K.) ;
* Correspondence e-mail: rameshkumarkuk@gmail.com, rameshchemkuk@kuk.ac.in (R.K.);
Scopus Author ID 35734222200
Received: 14.06.2023; Accepted: 16.11.2023; Published: 20.07.2024

Abstract: In the present investigation, polyacrylamide-coated magnetite nanoparticles (PAM-MNPs) were successfully synthesized through the chemical co-precipitation method and were employed to remove most consumable imidacloprid insecticide from the aqueous system through batch experiments. FTIR, FESEM, XRD, TGA, VSM, and UV-Vis analyses were used to analyze the synthesized nanoparticles' physio-chemical characteristics. The influencing factors, including pH, insecticide concentration, adsorbent dosage, contact duration, and temperature, were investigated for effective imidacloprid removal. The results indicated that 96.71% of the imidacloprid had been eliminated after 100 minutes. The experimental results of the adsorption kinetics were an excellent match with the pseudo-second-order kinetic model. Moreover, the Temkin adsorption isotherm model fits the adsorption isotherms better than the Freundlich and Langmuir model. Based on the thermodynamic investigation (free energy change, enthalpy change, and entropy change), the IMC insecticide adsorption process onto the surface of PAM-MNPs was exothermic and spontaneous. The reusability of these nano-adsorbents was further investigated using desorption tests. The results of these investigations showed that the polyacrylamide-coated magnetite nanoparticles possessed good adsorption capability, and these nanoadsorbent might be employed to treat wastewater that includes the insecticide imidacloprid as a lethal contaminant.

Keywords: adsorption; imidacloprid; magnetite nanoparticles; polyacrylamide.

1. Introduction

Pesticides are produced and used all over the world to control pests. The demand for agricultural goods has increased due to the tremendous increase in global population growth, and pesticides can resolve this problem by increasing crop yield [1]. Unfortunately, hazardous pesticide residues in soil, food, water, and the environment pose a threat to the overuse of pesticides. According to some estimates, only 1% of all pesticides are consumed by the targeted pests, while 99% are bioaccumulating throughout the food web [2,3]. Thus, pesticide residues must be eliminated from all-natural sources like soil and water. Pesticides are divided into

several categories and have various chemical compositions. Neonicotinoids are one of them and have been used to protect crops against insect pests. Neonicotinoids have recently surpassed all other classes of pesticides in terms of usage due to their better physicochemical characteristics and strong efficacy against insects. They control at least 25% of the global pesticide business today. Imidacloprid (IMC), clothianidin, dinotefuran, nitenpyram, and thiamethoxam are only a few examples of neonicotinoids [4,5]. The insecticide imidacloprid is used to eliminate harmful pests such as rice hoppers, aphids, leaf and plant hoppers, and whiteflies.

Additionally, it works well in the case of termites, soil insects, and a few breeds of biting insects like Colorado beetles and rice water weevils. Imidacloprid is used in various crops such as rice, cereals, cotton, maize, potatoes, sugar beet, vegetables, citrus fruit, stone fruit, and pome fruit for seed dressing, foliar treatments, and soil treatments. The organic insecticide imidacloprid, which is chlorinated, has a very negative effect on insects' central nervous systems [6].

Numerous techniques, including nano-membrane filtering, photocatalytic degradation, aeration degradation, advance oxidation, adsorption, and ozonation, have been developed so far to eliminate imidacloprid insecticide from wastewater. Some of these methods are inappropriate because they produce toxic by-products. Due to cheap operating costs, ease of use, and adaptability in design, eliminating the pesticide from wastewater by adsorption process is deemed the most effective approach among all those now in use [7,8]. Several experiments utilizing different adsorbents to remove imidacloprid from aqueous solutions have been published recently [9–16]. As a result of these investigations, we have employed polyacrylamide (PAM) coated magnetite nanoparticles to remove imidacloprid insecticide from the aqueous solution. We have also differentiated the outcomes of our investigation from those of previously published research against the elimination of IMC insecticide. Therefore, it is important to note that, after comparing with the previously reported conventional adsorbents, imidacloprid removal percentage utilizing polyacrylamide-modified magnetite (Fe_3O_4) nanoparticles was found to be greater. The impacts of several factors, including the amount of PAM-Fe_3O_4 nanoparticles, pH of the solution, imidacloprid initial concentration, and contact time on the elimination efficacy of IMC insecticide from the aqueous solution by PAM-Fe_3O_4 nanoparticles as an adsorbent material were investigated. Studies on the isotherm, kinetics, and thermodynamics were also carried out. Moreover, the outcomes of isotherm studies demonstrated that the adsorption process was in good agreement with the Temkin model.

Additionally, the kinetics study concluded that the adsorption process obeyed the pseudo-second-order kinetic model. The synthesized nano-adsorbents can also be recycled and reused many times for the adsorption of imidacloprid. As a result, the imidacloprid insecticide may be effectively and efficiently adsorbed from an aqueous solution using polyacrylamide-coated magnetite nanoparticles.

2. Materials and Methods

2.1. Chemicals used.

All of the chemicals used for this work, including ferrous sulfate heptahydrate ($FeSO_4.7H_2O$, 98 percent), ferric chloride hexahydrate ($FeCl_3.6H_2O$, 98 percent), NH_4OH

solution (25 percent), and polyacrylamide were bought by SRL (India). Throughout the experiment, analytically graded compounds were utilized with no additional purification.

2.2. Instruments.

Magnetic nanoparticles that were both uncoated and coated were synthesized using a digital overhead stirrer. The infrared spectra of magnetite nanoparticles that were uncoated and coated with polyacrylamide were identified using an ABB MB-3000 FTIR spectrometer. Perkin Elmer STA-6000 thermogravimetric analyzer was used to conduct the thermal examination of uncoated and coated nanoparticles. The mean size of bare and coated Fe_3O_4 nanoparticles was measured with the help of Hitachi SU-8000 FESEM. X-ray diffraction patterns were captured using source radiation with a wavelength of 1.5406Å drops at ambient temperature. The UV-Vis spectrophotometer T90 PG Instrument Limited measured the absorbance investigations.

2.3. Synthesis of Fe_3O_4 and PAM- Fe_3O_4 NPs.

Synthesis of iron oxide magnetic nanoparticles was carried out by co-precipitation method using a 100mL solution of the ferrous and ferric salts in the molar ratio 1:2 in the presence of nitrogen gas. After 30 minutes of stirring, precipitation was obtained by adding 20mL of NH_4OH solution and vigorously stirring at 85°C. pH of the reaction solution was between 9 and 10. The emergence of black color precipitates provided evidence that magnetite nanoparticles had been synthesized. After that, in 50mL of water, 0.5g of polyacrylamide was dissolved and added rapidly into the beaker containing magnetite nanoparticles with a further 1 hr continuous stirring. These synthesized PAM-MNPs were separated using an external magnet, rinsed thoroughly with deionized water, and dried in a vacuum oven at 25ºC.

2.4. Experiments to remove pesticide from aqueous solution.

Batch studies were used to investigate the pesticide adsorption by the PAM-MNPs at varied contact durations (10-120min), insecticide concentrations (10-50ppm), adsorbent dosage (from 5 to 30mg), and temperature (15-45ºC). Except for the tests in which the impact of the initial IMC concentration was examined, the initial IMC solution concentration for all batch studies was adjusted to 50ppm. Then, 10mL aqueous solution of the imidacloprid insecticide was added to a known mass of PAM-MNPs. The resulting suspension was quickly agitated (1500rpm), and the magnetic nanoadsorbent was removed from the above-used solution with an external magnetic field. UV-Vis spectrophotometer at λ_{max} 270nm was used to measure the pesticide concentration in the aqueous solution. The percentage removal efficiency and adsorption capacity were calculated using the following expressions [17]:

$$\%R = \frac{(C_o - C_e)100}{C_o}$$

$$q_e = \frac{(C_o - C_e)V}{m}$$

Where C_o and C_e, denote the initial IMC concentration and residual IMC concentration, respectively. The adsorbent mass, equilibrium adsorption capacity, and volume of the solution employed are denoted as m (g), q_e (mg/g), and V (L), respectively.

2.5. Desorption study.

A desorption experiment was conducted to determine whether PAM- Fe_3O_4 nanoparticles could be reused or not. Imidacloprid adsorbed over the surface of 30mg of Fe_3O_4 nanoparticles modified with polyacrylamide (IMC-PAM-Fe_3O_4 nanoparticles) was mixed with the desorbing solvent of 10mL volume at room temperature and agitated for approximately 120 minutes. A magnet was used to separate the PAM-Fe_3O_4 nanoparticles from the above-used IMC aqueous solution, and the decanted solution's absorbance was then measured at λ_{max} 270nm with the help of a UV-Vis spectrophotometer. The desorption percentage was determined using this equation [18]:

$$Desorption\ (\%) = \frac{C \times V}{qm} \times 100$$

Where, m represents the mass of IMC-PAM-Fe_3O_4 nanoparticles used, the volume of desorbing solvent employed is denoted by V (L), C (mg/L) represents the IMC insecticide concentration in the desorbing solvent, and q (mg/g) is the amount of IMC insecticide adsorbed onto the PAM-MNPs before the desorption study. PAM-MNPs were then separated and dried after desorption. Then, to determine whether these nanoparticles might be reused, the capacity of adsorption of recycled nanoparticles for IMC was examined again.

3. Results and Discussion

3.1.Characterization of Fe_3O_4 and PAM-MNPs.

PAM-MNPs were fabricated using the chemical co-precipitation method. TGA, FTIR, XRD, FESEM, and VSM techniques were used to characterize obtained nanoparticles (NPs).

3.1.1. FTIR study.

The FTIR spectra were used to confirm the successful coating of polyacrylamide over the surface of magnetite nanoparticles (Figure 1). In the Fe_3O_4 infrared spectrum, a peak at approximately 583 cm^{-1} appeared due to the stretching vibration of the Fe-O bond. Meanwhile, in the IR spectrum of PAM-MNPs, this peak was observed at approximately 560 cm^{-1}. Also, an absorption band at 3250-3450cm^{-1} in IR spectrum of PAM-MNPs was observed corresponding to the N-H stretching.

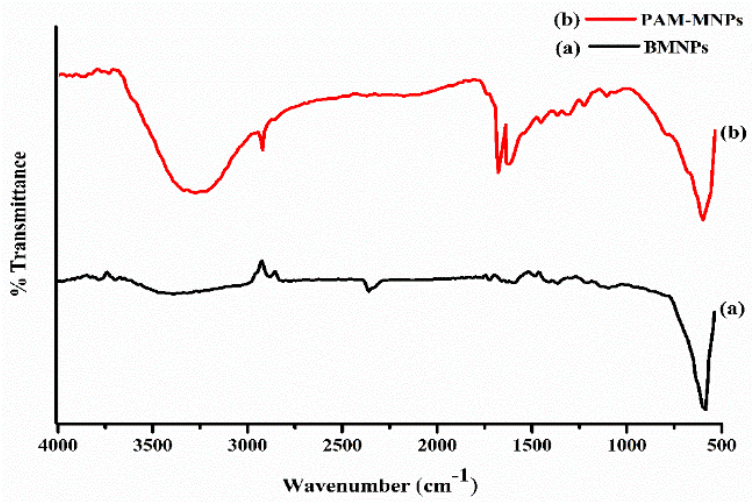

Figure 1. FTIR spectrum of **(a)** bare magnetite nanoparticles (BMNPs); **(b)** polyacrylamide modified magnetite nanoparticles (PAM-MNPs).

Meanwhile, the absorption bands at 2926 cm^{-1} and 1398 cm^{-1} are due to the stretching vibrations of the CH_2 groups and C-N stretching included in the macromolecular chains. Further bands due to stretching vibrations associated with the C=O of the amide group are visible at 1680cm^{-1}, while the shoulder peak at 1632cm^{-1} may be attributed to N-H bending vibrations. These distinctive PAM peaks proved that Fe_3O_4 had been effectively coated with PAM.

3.1.2. X-ray diffraction (XRD) study.

Diffractograms revealed the crystalline structure and crystallite sizes of the prepared nanoparticles. The XRD patterns of Fe_3O_4 and PAM-Fe_3O_4 nanoparticles were recorded (Figure 2). The Scherer's formula was used to determine the crystallite size with the help of the most intense peak of XRD:

$$d = \frac{0.9\lambda}{\beta cos\theta}$$

Where, d is the mean size of the particle, θ is the Bragg angle of a peak, λ is the X-ray source wavelength in nm, and β denotes the full width at half maximum (FWHM) of the most intense peak. The average crystallite sizes for bare Fe_3O_4 and PAM-coated Fe_3O_4 nanoparticles had been found to be 14.83 nm and 17.01 nm, respectively. Also, the crystallite size of Fe_3O_4 and PAM-coated magnetite nanoparticles obtained by the Debye Scherrer equation was very close to the FESEM analysis results. So, XRD and FESEM studies confirmed the size (in nm) of bare and coated MNPs.

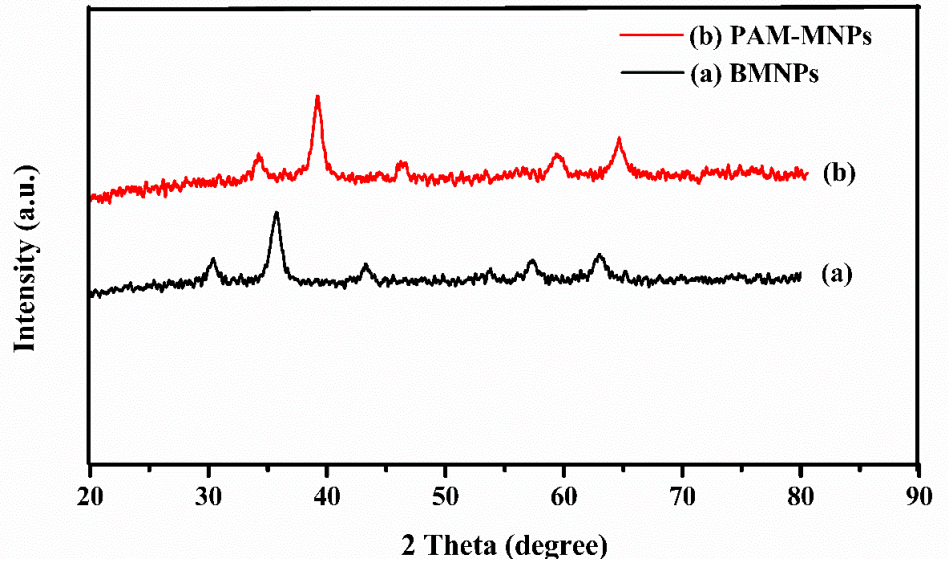

Figure 2. XRD patterns of **(a)** BMNPs; **(b)** PAM-MNPs.

3.1.3. Thermogravimetric (TGA) analysis.

TGA technique was employed to investigate the thermal behavior of synthesized coated and uncoated nanoparticles (Figure 3). Firstly, the weight loss below 150ºC for both coated and uncoated samples may result in moisture's evaporation. The second weight loss for the PAM-MNPs at 150–600ºC was about 13%, which indicates the degradation of the polyacrylamide coating. These comparative thermal study findings demonstrated that magnetite nanoparticles were effectively coated with polyacrylamide.

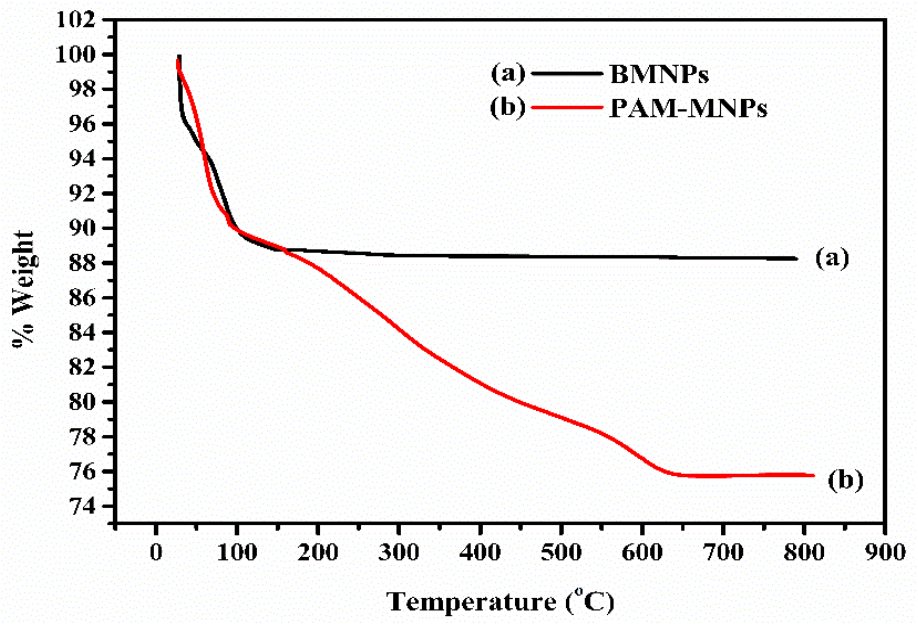

Figure 3. TGA curves of **(a)** BMNPs; **(b)** PAM-MNPs.

3.1.4. Field emission scanning electron microscopy (FESEM) study.

It was determined from the field emission electron microscopy (FESEM) analysis that the diameters of polyacrylamide-coated magnetite nanoparticles and naked magnetite nanoparticles were approximately 21.25 and 15.66nm, respectively (Figure 4). The increase in nanoparticles diameter also indicated that the magnetite nanoparticles' surface had been well coated with polyacrylamide.

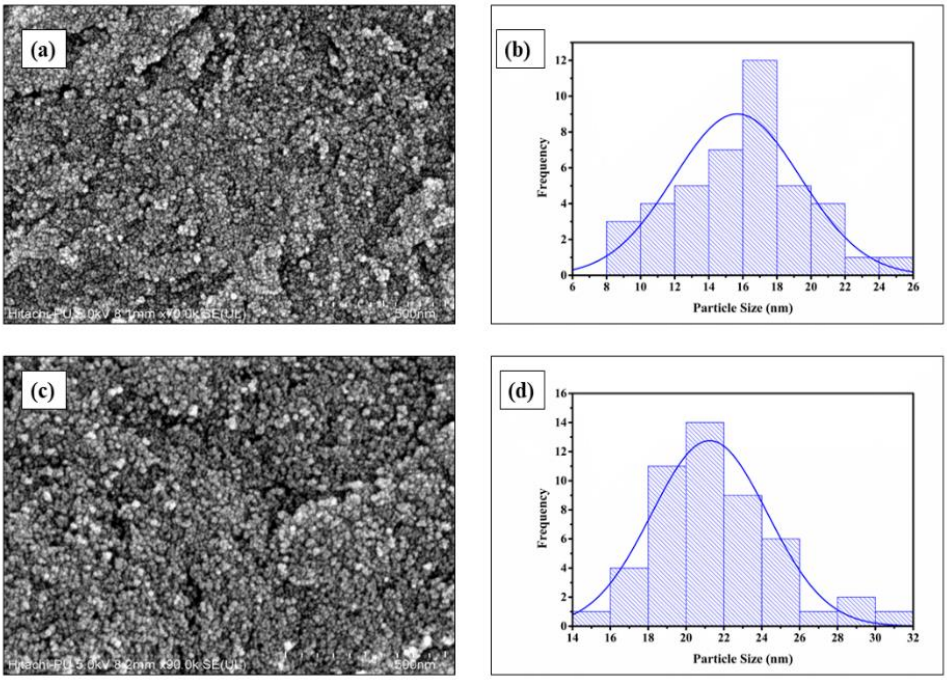

Figure 4. (a,b) FESEM micrograph of bare Fe_3O_4 nanoparticles with size distribution histogram; **(c,d)** FESEM micrograph of PAM coated Fe_3O_4 nanoparticles with size distribution histogram.

3.1.5 Magnetic properties.

The synthesized magnetic nanoparticles were analyzed by vibrating sample magnetometry. Figure 5 represents the hysteresis curve of polyacrylamide-coated Fe_3O_4 NPs and Fe_3O_4 NPs at 300K. Hysteresis loops verified the superparamagnetic behavior of both

Fe_3O_4 NPs and polyacrylamide-coated Fe_3O_4 NPs. The value of saturation magnetization (M_s) for the magnetite nanoparticles was determined to be equal to 61.862emu/g. Whereas the value of the saturation magnetization (M_s) for PAM-MNPs was 59.769emu/g, which was lower than that of bare MNPs. This behavior ensured the efficient PAM coating over the surface of bare Fe_3O_4 nanoparticles. The findings, however, demonstrated no appreciable decline in M_s value for the nanoparticles after polyacrylamide coating, indicating that the coating had no impact on the superparamagnetic behavior of the Fe_3O_4 NPs.

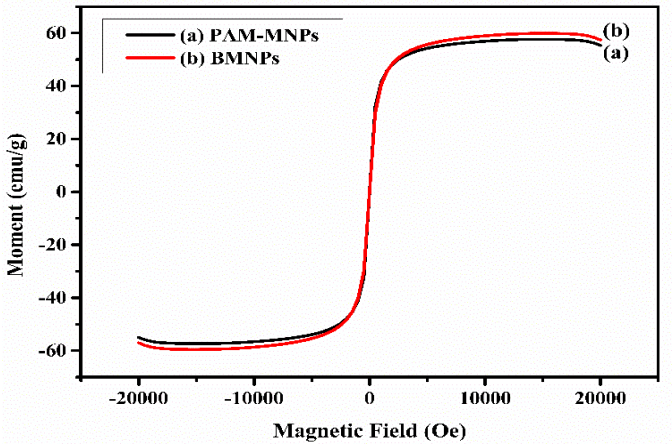

Figure 5. Magnetic hysteresis loops of **(a)** BMNPs; **(b)** PAM-MNPs at 300K.

3.2. Kinetic study for pesticide removal.

The kinetic study of the synthesized PAM-MNPs as an adsorbent for the elimination of imidacloprid insecticide from aqueous solutions was investigated by changing the parameters affecting adsorption capacity like the quantity of adsorbent, pH, IMC initial concentration, contact time, and temperature.

3.2.1. Influence of adsorbent dosage.

The removal efficiency of imidacloprid adsorbed by different adsorbent dosages is presented in Figure 6. Based on the outcomes of the adsorption experiment, the removal efficiency of PAM-MNPs increased from 79.57% to 96.71%, respectively, with an increment in the mass of the adsorbent from 5 mg to 30 mg. Hence, it was concluded that more adsorption sites were created by increasing the adsorbent dosage, indicating that more adsorbate was adsorbed over the surface of the adsorbent.

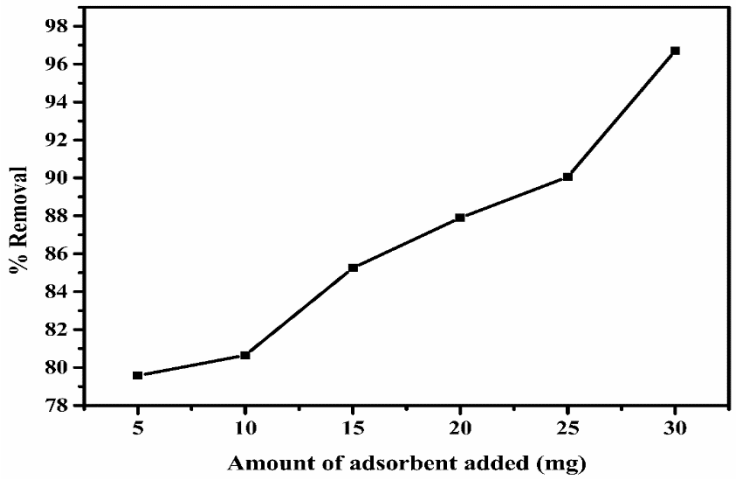

Figure 6. Influence of adsorbent dosage on the removal efficiency of IMC insecticide.

3.2.2. Influence of contact time.

Figure 7 shows the imidacloprid adsorption by PAM-MNPs at different contact periods in the solution with an initial IMC concentration of 50 ppm. The findings highlighted that the adsorption process was quick at the beginning of the adsorption process. Still, it slowed down near equilibrium due to less availability of adsorption sites with the passage of time. Figure 7 showed that the greatest removal efficacy was noticed at 100 minutes, which was 96.71%.

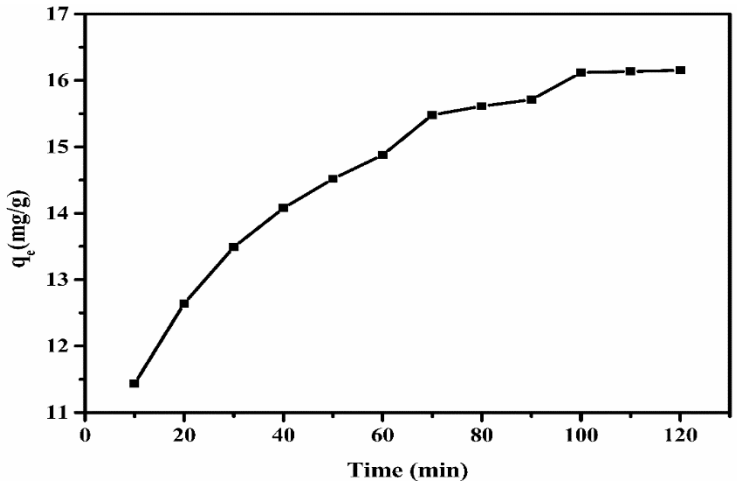

Figure 7. Adsorption efficiency of PAM-Fe_3O_4 NPs for IMC insecticide removal at different contact times.

3.2.3. Impact of initial IMC concentration.

Figure 8 displays the effectiveness of imidacloprid pesticide elimination by PAM-MNPs at different initial concentrations. The adsorption capability was seen to be decreased when the IMC concentration was raised progressively from 10 to 50 ppm. At low concentrations, the adsorption percentage was high due to the availability of vacant binding sites. However, when the initial IMC insecticide concentration was increased, the adsorption percentage decreased because the adsorbent surface binding sites became saturated.

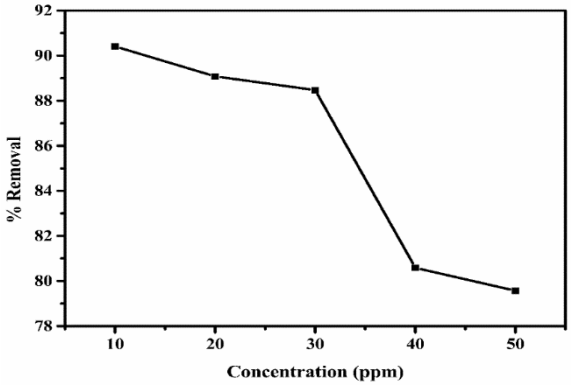

Figure 8. Impact of initial IMC concentration.

3.2.4. Impact of the pH.

The pH of the solution is crucial to the adsorption process because it may impact the adsorbate's and adsorbent's surface charges. According to Figure 9, the percentage adsorption efficiency of 30mg PAM-MNPs for 50ppm imidacloprid solution gradually increased with an increment in pH value from 2 to 7 and afterward decreased from 7-11. These findings revealed that, at pH 7, the maximum adsorption efficiency was noted due to the neutral condition of IMC. Thus, it is considered that the nano adsorbent exhibited exceptional adsorption capacity in neutral conditions. As we decreased pH from 7 to 2, adsorption decreased due to the

development of a positive charge on adsorbent and adsorbate which resulted in electrostatic repulsion between them. On the other hand, at pH 7, the strongest hydrogen bonds and electrostatic interactions between the adsorbent and adsorbate are responsible for the maximum adsorption of IMC on the surface of PAM-MNPs. Due to electrostatic repulsions among the negatively charged surfaces of the adsorbent and adsorbate at higher pH levels, the percentage of imidacloprid removal declined progressively. Therefore, it can be concluded that pH 7, the highest imidacloprid adsorption on the surface of the nano-adsorbent, was observed.

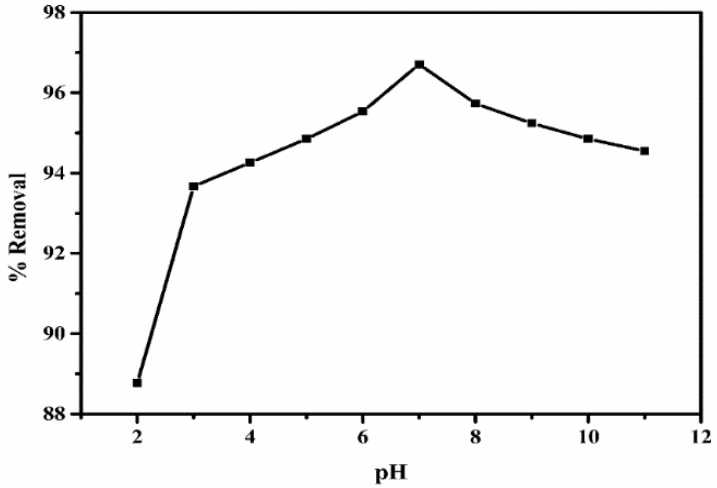

Figure 9 Impact of pH on IMC insecticide removal by PAM-Fe_3O_4 NPs.

3.2.5. Adsorption kinetic models.

Kinetic studies are crucial to the adsorption process and aid in examining how the adsorbent's capacity changes over time. Kinetic models explain the adsorption kinetics and probable mechanism involved. Moreover, a variety of kinetic models are available to study the adsorption mechanism. Based on these investigations, the pseudo-first-order and pseudo-second-order models were employed in this study to match the experimentally obtained kinetic data to understand the mechanism of IMC adsorption over the surface of PAM-Fe_3O_4 nanoparticle. The pseudo 1st order rate equation, also referred to as Lagergren's equation, is represented as follows [19]:

$$log(q_e - q_t) = logq_e - \frac{k_1 t}{2.303}$$

Where, q_e stands for the PAM-coated nanoparticle's equilibrium adsorption capacity, q_t stands for the PAM- Fe_3O_4 NPs adsorption efficiency at time t, and k_1 stands for the pseudo 1st order rate constant. The equation given below represents the pseudo-second-order kinetic model [20]:

$$\frac{t}{q_t} = \frac{1}{k_2 {q_e}^2} + \frac{t}{q_e}$$

Where k_2 is the pseudo 2nd order kinetic model's rate constant.

A summary of the kinetic analysis of PAM-MNPs' adsorption of IMC is depicted in Table 1. According to these results, the removal of IMC by PAM-MNPs coincides with the 2nd-order kinetic model by using correlation coefficient (R^2) values to infer the occurrence of the chemisorption process (Figure 10).

Table 1. Kinetic parameters for the IMC insecticide adsorption on PAM- Fe_3O_4 NPs.

Pseudo first order kinetic model			**Pseudo second order kinetic model**		
R^2	k_1 (min^{-1})	q_e (mg/g)	R^2	k_2 (g $mg^{-1}min^{-1}$)	q_e (mg/g)
0.984	.031	6.779	0.998	0.009	16.744

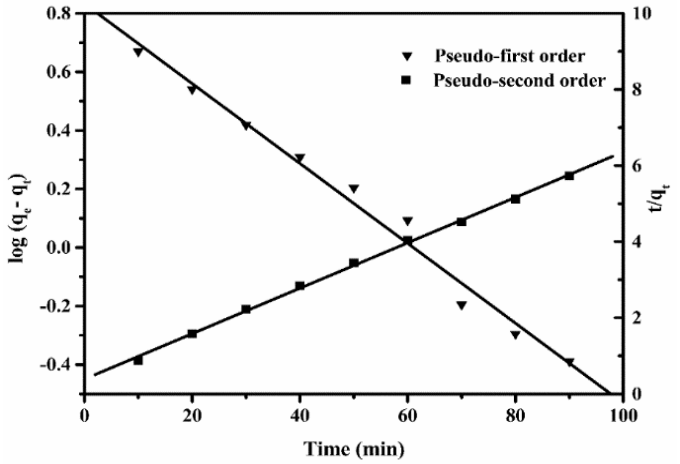

Figure 10. Pseudo 1st order kinetic plot and pseudo 2nd order kinetic plot for adsorption of IMC insecticide on PAM-Fe_3O_4 NPs.

3.2.6. Adsorption isotherm models.

The design of an adsorption system depends on the equilibrium adsorption isotherm, which is vital in characterizing the interaction behavior between solutes and adsorbent. To understand the nonlinear equilibrium connection between the solute adsorbed over the adsorbent and that remaining in the solution, several isotherm models, including Langmuir, Freundlich, and Temkin, were used. Three widely used adsorption isotherm models, Langmuir, Freundlich, and Temkin, were utilized in this study to examine the adsorption data. The Langmuir isotherm's linear form is represented as follows [21]:

$$\frac{C_e}{q_e} = \frac{1}{q_m K_L} + \frac{C_e}{q_m}$$

Where, Langmuir adsorption equilibrium constant (K_L) is connected to the adsorption energy and the q_m (mg/g) represents the surface concentration at monolayer coverage, the greatest value of q_e may be reached when C_e is raised. From the plot of (C_e/q_e) vs C_e in a linear regression, we can determine the values of K_L and q_m. The Freundlich isotherm's linear form is shown as follows [22]:

$$\log q_e = \log K_F + \frac{1}{n} \log C_e$$

Where K_F and n represent the Freundlich equation constants. The adsorbent's capacity for the adsorbate is represented by the constant K_F, and the adsorption distribution is related to n. The K_F and n values are derived from a linear regression graph of log q_e vs log C_e.

The following is a linear expression of the Temkin relationship [23]:

$$q_e = k_1 \ln k_2 + k_1 \ln C_e$$

Where k_2 stands for the equilibrium binding constant in L/mg, k_1 (RT/b) stands for the heat of adsorption, and b stands for the Temkin constant. It is possible to derive the values of k_1 and k_2 from the linear graph of q_e against ln C_e (Figure 11). The constants for each isotherm and the accompanying correlation coefficients are summarized in Table 2. The Temkin isotherm's correlation coefficient was higher than the Langmuir and Freundlich isotherms. This suggests that the Temkin model better describes the adsorption of IMC insecticide on PAM-MNPs.

Table 2. Calculated isotherm parameters values from different isotherm model for adsorption of IMC insecticide on PAM- Fe_3O_4 NPs.

Langmuir Isotherm Model			**Freundlich Isotherm Model**			**Temkin Isotherm Model**		
R^2	q_m	K_L	R^2	K_F	1/n	R^2	k_1	k_2
0.966	111.982	0.215	0.950	20.916	0.594	0.976	24.816	2.119

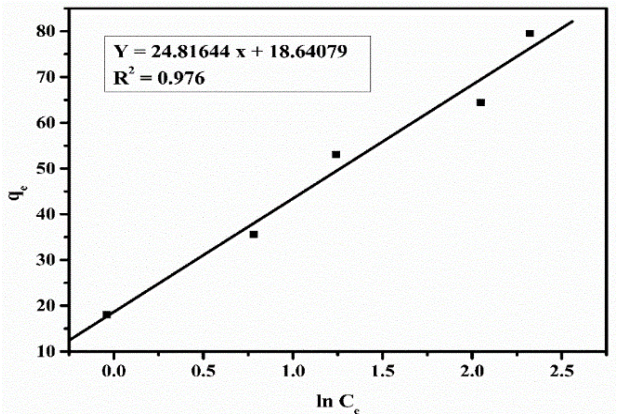

Figure 11. Temkin isotherm model.

3.2.7. Adsorption thermodynamics.

Thermodynamic analysis demonstrates the feasibility of the adsorption method. The impact of temperature on the removal of IMC insecticide onto the surface of PAM-MNPs from the aqueous solution was investigated at 15, 25, and 35ºC, respectively. When the temperature was raised from 15 to 35ºC, the elimination efficiency was improved, inferring that the IMC adsorption process onto the surface of these NPs may be kinetically regulated. The equilibrium constant (K_c) of the adsorption research was determined using the equation below based on the results of the experiments.

$$K_c = \frac{q_e}{C_e}$$

Where, C_e denotes the equilibrium IMC insecticide concentration in the solution (ppm), and q_e denotes the quantity adsorbed onto the PAM-Fe_3O_4 NPs at equilibrium (mg/g). The following equations were employed to determine the thermodynamic parameters like the standard enthalpy change (ΔH°), standard Gibbs energy change (ΔG°), and the standard entropy change (ΔS°), using experimentally collected data at various temperatures:

$$\Delta G^{\circ} = -RTlnK_c$$

$$lnK_c = \frac{-\Delta H^{\circ}}{RT} + \frac{\Delta S^{\circ}}{R}$$

Where R stands for the universal gas constant (R = 8.314J/mol K), K_C represents the equilibrium constant, and T stands for the absolute temperature (K) [24]. The slope and intercept for the graph of ln K_C versus 1/T provided the values of ΔH° and ΔS° (Figure 12). Table 3 presents the thermodynamic parameters of the IMC adsorption on the surface of PAM-Fe_3O_4 nanoparticles. The standard Gibbs free energy change measurements that are negative at different temperatures indicate that the adsorption of IMC by PAM-MNPs is spontaneous. The exothermic nature of the adsorption is implied by the standard enthalpy's negative value. The positive value of standard entropy change indicates the increasing randomness at the interface of solid/liquid during the adsorption of IMC on the synthesized NPs.

Table 3. Thermodynamics parameters of IMC insecticide adsorption on PAM- Fe_3O_4 NPs at various temperatures.

Temperature (K)	ΔG° (KJ/mol)	ΔHº (KJ/mol K)	ΔSº (J/K mol)
298	-5.653	-120.899	421.804
308	-7.856		
318	-14.176		

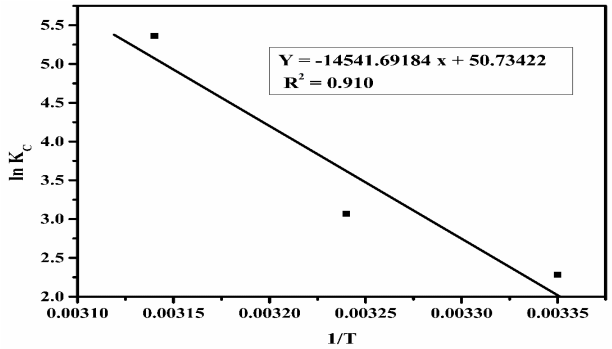

Figure 12. Plot of ln K_C vs 1/T for calculation of thermodynamics parameters.

3.3. Comparative adsorption capacities of IMC by PAM-MNPs with already reported adsorbent materials.

In our investigation, PAM-MNPs showed better adsorption ability for imidacloprid insecticide removal than the other already reported adsorbent materials (

Table 4). As a result, the polyacrylamide-coated magnetite nanoparticles utilized in this study have demonstrated tremendous potential to be an efficient adsorbent material for eliminating IMC insecticide from aqueous solutions. Therefore, it may be concluded that proper surface functionalization of nanomaterials would further improve their ability to remove emerging contaminants in wastewater.

Table 4. Comparative study of the percentage removal of IMC insecticide by the PAM-MNPs with adsorbents reported in **the** literature.

Sr. No.	Adsorbents used for IMC removal from aqueous solution	% Removal of IMC	Reference
1.	Poly(4,4'-methylenedianiline)/graphene oxide	66.7%	[9]
2.	Cement kiln dust	91%	[10]
3.	Eucalyptus woodchip-derived biochar	10.11%	[11]
4.	TiO_2 nanoparticles	90.24%	[12]
5.	Activated carbon	85%	[13]
6.	Silver@graphene oxide nanocomposite	63%	[14]
7.	Chitosan	40%	[15]
8.	Chitosan functionalized AgNPs	85%	[15]
9.	Activated carbons from agricultural waste	80%	[16]
10.	**PAM-MNPs**	**96.71%**	**Present work**

3.4. Desorption analysis.

A desorption study was conducted to assess adsorbent regeneration and adsorbate recovery. The desorption investigation showed that after 120 minutes, a maximum of 89% of the IMC insecticide was desorbed from the surface of the PAM-MNPs. Furthermore, no discernible change in the recycled PAM-Fe_3O_4 nanoparticles' ability to adsorb pesticide from an aqueous solution was seen, suggesting that these nanoparticles may be employed again to further eliminate IMC residues from polluted water.

4. Conclusion

The chemical co-precipitation method was employed to synthesize polyacrylamide-coated Fe_3O_4 nanoparticles, which were then used to adsorb the insecticide imidacloprid. Numerous physicochemical analyses pointed towards the excellent surface coating of Fe_3O_4 nanoparticles with coating material. Adsorption of imidacloprid varies with changes in several factors, including adsorbent dosage, contact duration, pH, starting concentration of IMC, and temperature, according to batch adsorption experiments. The imidacloprid adsorption over the surface of PAM-Fe_3O_4 nanoparticles appeared to follow pseudo-second-order kinetics in agreement with the adsorption kinetics data. The Temkin isotherm model was found to be best fitted, as revealed by the adsorption isotherm data. The desorption investigation study confirmed that the synthesized nano-adsorbent can be reused again to remove the imidacloprid insecticide. Therefore, it can be inferred from the current work that PAM-Fe_3O_4 nanoparticles are a viable adsorbent tool for eliminating insecticide from wastewater and are a more efficient adsorbent than any other reported adsorbent material.

Funding

Co-author (Keerti Rani) is also highly obliged to UGC in New Delhi, India, for offering financial help as a Senior Research Fellowship. (Award no. NOV2017-114450).

Acknowledgment

All authors appreciate Kurukshetra University for providing the necessary research facilities.

Conflicts of Interest

All authors proclaim to have no conflict of interest.

References

1. Gecgel, C.; Simsek, U.B.; Turabik, M. Degradation of imidacloprid in aqueous solutions by zero valent iron nanoparticles in the nitrogen medium. *Desalin. Water Treat.* **2018**, *114*, 341–355, http://doi.org/10.5004/dwt.2018.22355.
2. Sellaoui, L.; Gómez-Avilés, A.; Dhaouadi, F.; Bedia, J.; Bonilla-Petriciolet, A.; Rtimi, S.; Belver, C. Adsorption of emerging pollutants on lignin-based activated carbon: Analysis of adsorption mechanism via characterization, kinetics and equilibrium studies. *Chem. Eng. J.* **2023**, *452*, 139399, http://doi.org/10.1016/j.cej.2022.139399.
3. Goh, P.S.; Lau, W.J.; Ismail, A.F.; Samawati, Z.; Liang, Y.Y.; Kanakaraju, D. Microalgae-Enabled Wastewater Treatment: A Sustainable Strategy for Bioremediation of Pesticides. *Water* **2023**, *15*, 70, http://doi.org/10.3390/w15010070.
4. Guo, L.; Tian, M.; Wang, L.; Zhou, X.; Wang, Q.; Hao, L.; Wu, Q.; Wang, Z.; Wang, C. Synthesis of hydroxyl-functional magnetic hypercrosslinked polymer as high efficiency adsorbent for sensitively detecting neonicotinoid residues in water and lettuce samples. *Microchem. J.* **2023**, *187*, 108412, http://doi.org/10.1016/j.microc.2023.108412.
5. Pietrzak, D.; Kania, J.; Kmiecik, E.; Malina, G.; Wątor, K. Fate of selected neonicotinoid insecticides in soil–water systems: Current state of the art and knowledge gaps. *Chemosphere* **2020**, *255*, 126981, http://doi.org/10.1016/j.chemosphere.2020.126981.
6. Zhao, R.; Ma, X.; Xu, J.; Zhang, Q. Removal of the pesticide imidacloprid from aqueous solution by biochar derived from peanut shell. *BioRes.* **2018**, *13*, 5656–5669, http://doi.org/10.15376/biores.13.3.5656-5669.
7. Ghosh, N.; Das, S.; Biswas, G.; Haldar, P.K. Review on some metal oxide nanoparticles as effective adsorbent in wastewater treatment. *Water Sci. Technol.* **2022**, *85*, 3370–3395, http://doi.org/10.2166/wst.2022.153.

8. Shah, A.; Shah, M. Characterisation and bioremediation of wastewater: A review exploring bioremediation as a sustainable technique for pharmaceutical wastewater. *Groundw. Sustain. Dev.* **2020**, *11*, 100383, http://doi.org/10.1016/j.gsd.2020.100383.
9. Toolabi, A.; Mohseni, E.; Zare, M.R.; Mengelizadeh, N.; Rostami, E.; Taghavig, M.; Kharazi, S. Effective removal of diazinon and imidacloprid toxins from aqueous samples by nano poly(4,4′-methylenedianiline)/graphene oxide. *Desalin. Water Treat.* **2021**, *232*, 187–197, http://doi.org/10.5004/dwt.2021.27516.
10. El Refaey, A.A.E.K.; Abou-Elnasr, H. Comparative Study for Removal of Imidacloprid and Oxamyl Pesticides by Cement Kiln Dust: Kinetics and Equilibrium Studies. *Alexandria Sci. Exch. J.* **2022**, *43*, 459–470, http://doi.org/10.21608/asejaiqjsae.2022.255604.
11. Srikhaow, A.; Chaengsawang, W.; Kiatsiriroat, T.; Kajitvichyanukul, P.; Smith, S.M. Adsorption Kinetics of Imidacloprid, Acetamiprid and Methomyl Pesticides in Aqueous Solution onto Eucalyptus Woodchip Derived Biochar. *Minerals* **2022**, *12*, 528, http://doi.org/10.3390/min12050528.
12. Akbari Shorgoli, A.; Shokri, M. Photocatalytic degradation of imidacloprid pesticide in aqueous solution by TiO_2 nanoparticles immobilized on the glass plate. *Chem. Eng. Commun.* **2017**, *204*, 1061–1069, http://doi.org/10.1080/00986445.2017.1337005.
13. Lu, J.; Zhang, Z.; Lin, X.; Chen, Z.; Li, B.; Zhang, Y. Removal of imidacloprid and acetamiprid in tea (*Camellia sinensis*) infusion by activated carbon and determination by HPLC. *Food Control* **2022**, *131*, 108395, http://doi.org/10.1016/j.foodcont.2021.108395.
14. Keshvardoostchokami, M.; Bigverdi, P.; Zamani, A.; Parizanganeh, A.; Piri, F. Silver@ graphene oxide nanocomposite: synthesize and application in removal of imidacloprid from contaminated waters. *Environ. Sci. Pollut. Res.* **2018**, *25*, 6751–6761, http://doi.org/10.1007/s11356-017-1006-y.
15. Moustafa, M.; Abu-Saied, M.A.; Taha, T.; Elnouby, M.; El-shafeey, M.; Alshehri, A.G.; Alamri, S.; Shati, A.; Alrumman, S.; Alghamdii, H.; Al-Khatani, M. Chitosan functionalized AgNPs for efficient removal of Imidacloprid pesticide through a pressure-free design. *Int. J. Biol. Macromol.* **2021**, *168*, 116–123, http://doi.org/10.1016/j.ijbiomac.2020.12.055.
16. Mohammad, S.G.; El-Sayed, M.M.H. Removal of imidacloprid pesticide using nanoporous activated carbons produced via pyrolysis of peach stone agricultural wastes. *Chem. Eng. Commun.* **2021**, *208*, 1069–1080, http://doi.org/10.1080/00986445.2020.1743695.
17. Debebe, Y.; Alemayehu, E.; Worku, Z.; Bae, W.; Lennartz, B. Sorption of 2,4-Dichlorophenoxyacetic Acid from Agricultural Leachate Using Termite Mound Soil: Optimization Using Response Surface Methodology. *Water* **2023**, *15*, 327, http://doi.org/10.3390/w15020327.
18. Abate, G.Y.; Alene, A.N.; Habte, A.T.; Addis, Y.A. Adsorptive Removal of Basic Green Dye from Aqueous Solution Using Humic Acid Modified Magnetite Nanoparticles: Kinetics, Equilibrium and Thermodynamic Studies. *J. Polym. Environ.* **2021**, *29*, 967–984, http://doi.org/10.1007/s10924-020-01932-3.
19. Jianlong, W.; Xinmin, Z.; Decai, D.; Ding, Z. Bioadsorption of lead(II) from aqueous solution by fungal biomass of *Aspergillus niger*. *J. Biotechnol.* **2001**, *87*, 273–277, http://doi.org/10.1016/S0168-1656(00)00379-5.
20. Febrianto, J.; Kosasih, A.N.; Sunarso, J.; Ju, Y.-H.; Indraswati, N.; Ismadji, S. Equilibrium and kinetic studies in adsorption of heavy metals using biosorbent: A summary of recent studies. *J. Hazard. Mater.* **2009**, *162*, 616–645, http://doi.org/10.1016/j.jhazmat.2008.06.042.
21. Kamali, M.; Esmaeili, H.; Tamjidi, S. Synthesis of Zeolite Clay/Fe-Al Hydrotalcite Composite as a Reusable Adsorbent for Adsorption/Desorption of Cationic Dyes. *Arab. J. Sci. Eng.* **2022**, *47*, 6651–6665, http://doi.org/10.1007/s13369-022-06580-4.
22. Rizzi, V.; Gubitosa, J.; Fini, P.; Romita, R.; Agostiano, A.; Nuzzo, S.; Cosma, P. Commercial bentonite clay as low-cost and recyclable "natural" adsorbent for the Carbendazim removal/recover from water: Overview on the adsorption process and preliminary photodegradation considerations. *Colloids Surfaces A Physicochem. Eng. Asp.* **2020**, *602*, 125060, http://doi.org/10.1016/j.colsurfa.2020.125060.
23. Dada, A.O.;Olalekan, A.P.; Olatunya, A.M.; Dada, O. Langmuir, Freundlich, Temkin and Dubinin–Radushkevich Isotherms Studies of Equilibrium Sorption of Zn^{2+} Unto Phosphoric Acid Modified Rice Husk. *IOSR J. Appl. Chem.* **2012**, *3*, 38–45, http://doi.org/10.9790/5736-0313845.
24. Ali, N.S.; Jabbar, N.M.; Alardhi, S.M.; Majdi, H.S.; Albayati, T.M. Adsorption of methyl violet dye onto a prepared bio-adsorbent from date seeds: isotherm, kinetics, and thermodynamic studies. *Heliyon* **2022**, *8*, e10276, http://doi.org/10.1016/j.heliyon.2022.e10276.